

Los Alamos National Laboratory is operated by the University of California for the United States Department of Energy under contract W-7405-ENG-36.

DEC 13 1983

OSTI

TITLE: EFFECTS OF STRUCTURAL SETTING AND ROCK PROPERTIES ON AMPLITUDES OF SURFACE MOTIONS IN THE VICINITY OF SMALL EXPLOSIVE TESTS

AUTHOR(S): C.L. EDWARDS
D. CRAIG PEARSON
DIANE F. BAKER
CATHY AIMONE-MARTIN

SUBMITTED TO:

DISCLAIMER

This report was prepared as an account of work sponsored by an agency of the United States Government. Neither the United States Government nor any agency thereof, nor any of their employees, makes any warranty, express or implied, or assumes any legal liability or responsibility for the accuracy, completeness, or usefulness of any information, apparatus, product, or process disclosed, or represents that its use would not infringe privately owned rights. Reference herein to any specific commercial product, process, or service by trade name, trademark, manufacturer, or otherwise does not necessarily constitute or imply its endorsement, recommendation, or favoring by the United States Government or any agency thereof. The views and opinions of authors expressed herein do not necessarily state or reflect those of the United States Government or any agency thereof.

MASTER

By acceptance of this article, the publisher recognizes that the U.S. Government retains a nonexclusive, royalty-free license to publish or reproduce the published form of this contribution, or to allow others to do so, for U.S. Government purposes.

The Los Alamos National Laboratory requests that the publisher identify this article as work performed under the auspices of the U.S. Department of Energy.

DISTRIBUTION OF THIS DOCUMENT IS UNLIMITED

Los Alamos Los Alamos National Laboratory
Los Alamos, New Mexico 87545

**EFFECTS OF STRUCTURAL SETTING AND ROCK PROPERTIES
ON AMPLITUDES OF SURFACE MOTIONS IN THE VICINITY
OF SMALL EXPLOSIVE TESTS**

by

C. L. Edwards
Los Alamos National Laboratory
Los Alamos, New Mexico 87545

D. Craig Pearson
Los Alamos National Laboratory
Los Alamos, New Mexico 87545

Diane F. Baker
Los Alamos National Laboratory
Los Alamos, New Mexico 87545

Cathy Aimone-Martin
New Mexico Institute Of Mining and Technology
Socorro, New Mexico 87801

ABSTRACT

A series of small-scale explosive experiments were conducted in a perlite mine near Socorro, New Mexico. These experiments were a joint effort between Los Alamos National Laboratory, New Mexico Institute Of Mining and Technology, Southern Methodist University, and Defense Nuclear Agency. The purpose of these tests was to measure the changes in the shock wave and seismic coupling as a function of depth of burial and structural setting. The size of the explosive charges ranged from 1 to 68 kg. Over 1150 measurements of velocity and acceleration were made on thirteen experiments using three component sensors. The sensors were placed to maximize the azimuthal coverage as well as to provide data at a variety of ranges from ~1 to 130 m. A few far field measurements were made at ranges of ~2 km. While the bulk of the measurements were made on the surface, high g accelerometers were placed in one instrumentation borehole to provide some free-field measurements. Preliminary results indicate that significant differences in the amplitudes of signals can occur when the location of the explosive charges are changed by only meters. Part of the observed difference is attributed to variations in the rock immediately adjacent to the charge affecting the shock coupling; and part to the effects of the site characteristics.

Tables and figures follow text.

INTRODUCTION

Ground motion analysis has been a key part of the Los Alamos Source Region Program (SRP) for several reasons: near-source ground motion represents the up-going energy from an explosion and that information is required to assess the total energy budget for an explosion. A large number of measurements both inside and outside the spall region is key to understanding the complexity of the signals. Spall results from the tensile failure of surficial material resulting in vertical detachment of the material from the earth. These data can be used to benchmark the numerical modeling of the nonlinear zone. Last, but not least, later time phenomena, such as spall closure, are believed to play significant roles in seismic and other signals used for detection, discrimination, and characterization of underground explosions. As a result, characterization of close-in ground motions in different media has been a major goal of the Source Region Program.

One of the topics being addressed by the SRP is the three-dimensional characterization of the spall volume as a function of time (size, shape, volume, mass, ground motions, surface expression, and degree of damage). Surface observations of acceleration, velocity, and displacement provide constraints for spall and, when combined with the limited amount of subsurface ground-motion data (not presented in this report), allow a three-dimensional model to be generated.

Presented herein are the data and preliminary results from a variety of close-in ground-motion experiments conducted by Los Alamos and its collaborators (New Mexico Institute of Mining and Technology (New Mexico Tech), Southern Methodist University and the Defense Nuclear Agency, Albuquerque) on the 13 small-scale (1 to 68 kg) charges.

EXPERIMENT SITE

The experiments were conducted in the Dicaperl Perlite Mine located three miles southwest of Socorro, New Mexico, at the southeastern edge of the Socorro Mountains. Perlite is a hydrated volcanic glass that is heated and expanded to form a product used as a filter material. The silica content of this deposit is 76% with a 3.4% water content. Mine production is 240,000 tons of ore per year with estimated reserves of 12,000,000 tons.

The Dicaperl dome was formed 7.4 million years ago. The deposit has a domed shape, exhibits depositional flow banding, and is faulted on the east side and eroded on the top. Dominant joint sets trend in north-south and west northwest-east southeast directions. We also measured fracture orientations exposed at the surface of the mine floor where the experiments were performed (Figure 1). The major axis is parallel to the long axis of the instrumentation array (about 0°), with a secondary set striking about 90° . The dome's horizontal extent is 610 m wide by 790 m long and has an exposed vertical extent of 140 m with thickness ranging from 90 to over 150 m.

The perlite body was deposited as an extrusive, rhyolitic lava with a high silica content and hence, high viscosity. Crystallization did not occur and obsidian was formed when the lava cooled rapidly by contact with the surrounding rocks. The interior of the dome cooled by vesiculation, leaving a solid core of obsidian. The Dicaperl dome has a surface layer of

crystalline rock on the northeast edge that may have formed during an earlier period of slow cooling at depth before rising or being pushed to the surface.

The perlite formed through rapid and thorough hydration of the obsidian core. The elongated shape, a result of the north-south lava flow direction, and closely packed nature of the vesicles, provided paths for meteoric water to travel resulting in hydration of the glass. The hydration of the glass occurred as a low temperature diffusion process as water migrated inward through fractures and vesicles that provided the surface area for the hydration to progress.

Figure 2 shows an aerial photograph of the portion of the mine that was used for these experiments. The shotholes and sensor locations are superimposed on the photograph.

A seismic refraction survey was conducted to estimate the near-surface seismic velocities in the perlite. The interpretation was performed using first-arrival travel times only. A commercial refraction interpretation package called GREMIX was used to assist in the interpretation. This software is basically an implementation of the Generalized Reciprocal Method. It provides a good estimate of the depth to a refracting horizon, but does not attempt to model vertical variations in velocity with the exception of those due to layering (that is, vertical velocity variations within a layer are not modeled).

The apparent velocities on either side of the central source location are slightly different, but both are higher than the near-surface apparent velocities measured from end shots, which are quite low at 350 m/s. Such low velocities are characteristic of dry, unconsolidated porous materials. The velocity of the refracting horizon is 1335 m/s; the depth to this refractor varies from 4 to 10 m below ground surface. We suspect that this refractor simply represents the "normal" (unweathered) velocity for the perlite or alternatively, water saturation at this depth.

We measured the physical and elastic properties of several core samples taken near-surface in the experiment area. These results are summarized in Tables 1 and 2. We also measured the compressional wave velocities on several core samples in an attempt to further understand the velocity structure (Table 3). The results indicate significant variation in the velocities depending on the orientation parallel to or perpendicular to the flow banding.

EXPERIMENT DESIGN

The first seven experiments (P1-P7) utilized small charges (1-3 kg) in order to minimize the damage to the surrounding test bed. We wanted to determine the cratering curve for this particular rock and to obtain some preliminary measurements of seismic velocities and ground motion amplitudes.

The size of the charges in the following experiments needed to be large enough to produce significant ground motions. In addition, to model the results as a spherical explosion we wanted to have an aspect ratio less than 2.0. The final charge size was a cylinder 0.3 m in diameter and 0.6 m high, weighing 68 kg. Pertinent data about the individual shots are summarized in Table 4.

MEASUREMENT TYPES

Three types of ground motion measurements were performed on these experiments: 1) high g (25 g and 100 g) measurements in and near the spall region on the surface and in boreholes; 2) extended surface accelerometer measurements (to define and characterize the spall zone); and 3) velocity measurements well beyond spall. Not all types were used on each experiment. The first seven experiments were primarily designed to determine the cratering curve for perlite and to aid in the design of the heavily instrumented 68 kg charge experiments. All three types of measurements were made on experiments P8-P13.

High g Surface and borehole Accelerometer Measurements. These sensors were located within 15 m of surface ground zero for shots P9, P10, and P11. Each station typically recorded three components (vertical, radial, and tangential) of motion at ranges of 5, 10, 20, 30, and 40 m along seven different azimuths.

These sensors were also recorded on shots 8, 12, and 13 although they were located outside spall. The accelerometers used for these stations are Endevco 100-g or 25-g instruments (Endevco Model 2262), depending on the anticipated motions. The positive directions on the data plots presented herein are: vertical, up; radial, toward SGZ; and tangential, left of SGZ.

Extended Surface Accelerometer Measurements. For shots P11, P12, and P13 we acquired ground-motion data that straddled the edge of predicted spall and for all shots, data out to at least three times the predicted spall radius was recorded. To acquire these measurements, we installed portable stations consisting of accelerometers, portable power (batteries), and portable digital recorders. The accelerometers were: Model SA-111 force-balanced accelerometers (built by Terra Technology).

All accelerometer data were recorded by 25 6-channel Reftek DAS (data acquisition subsystems, made by Refraction Technology). We have preprocessed the data, which may include corrections for timing, amplitude calibration, baseline offsets, integration ramps, noise, etc. The data were recorded at 500 samples per second.

Extended Surface Velocity Measurements. New Mexico Tech personnel installed a linear array of velocity transducers beginning outside spall, interspersed with and extending to the edge of the linear portion of the accelerometer array.

The sensors were three component Geospace velocity sensors. The digital recording system (NOMIS) records 33 channels in an 8 bit format. Data were recorded at 1024 samples per second.

SURFACE MOTION DATA

The purpose of the first seven shots (P1-P7) was to confirm that the standard cratering curves were valid for this particular rock type, to determine the near surface compressional wave velocities, and to determine the range dependence of peak ground motion. We fielded the NOMIS velocity array on each shot. On shots P6 and P7, we fielded accelerometers and sensitive velocity gauges to confirm our computer determined sensitivities and gains for the fully instrumented experiments.

The primary purpose of P8 was to provide a comprehensive check of the complete instrumentation array at ground motions near what they would be in experiments P9, P10, P11, P12, and P13. Following the evaluation of the data from P8, the final instrument placement could be determined and the data acquisition parameters could be set with high confidence. Additionally, we would acquire ground motion data at a variety of ranges to well beyond the edge of spall and ground motion data at a variety of azimuths.

The primary purpose of experiments P9, P10, and P11 was to provide a extensive set of ground motion measurements on 68 kg explosive charges at three different scale depths. The explosive charges were fired at 40, 30, and 20 m in the same shot hole. We acquired ground motion data at a variety of ranges and azimuths from ground zero to well beyond the edge of spall. Figure 3 gives the geometry of these three experiments. Figure 4 is the slant range/time record sections of the long linear array ground motions. Figure 5 presents constant range variable azimuth record sections for shot P9.

The primary purpose of P12 and P13 was to provide a extensive set of ground motion measurements on 68 kg explosive charges located at the edges of mine floor. This provides additional data in the 40 to 150 m ranges with a different source location. The data presented here relates to the core experiments only, i.e. P9, P10, and P11.

PRELIMINARY CONCLUSIONS

Experiments P1 scaled depth of burial (SDOB 1.8 m/kg^{1/3}) and P2 (SDOB 1.6) produced RETARCs. A RETARC is a non-cratering of surface materials but bulking of the material to form a convex dome at the surface (crater spelled backwards). Experiments P3 (SDOB 1.1), P6 (SDOB 1.0), and P7 (SDOB 1.0) all produced throw out craters. P4 (SDOB 2.0) did not produce a RETARC, but there were several fractures, radiating out from the borehole, produced. P5 (SDOB 2.3) was the most deeply buried shot and produced no visible surface effects. These lightly instrumented shots allowed us to develop realistic recording parameters for the following shots.

Shots P9, P10, and P11 produced ground motions at all stations with good signal to noise. The geometry imposed by the various source depth-of-burials complicates the interpretation of single component data shown in this study. Further analysis, including all three components of ground motion, is necessary to separate the geometric effects from the structural effects. There is a strong indication of azimuthal variation in rock properties at the Grefco Dicapertl Mine. Spall initiation, dwell time, and range vary strongly as a function of azimuth. Future experiments at this site will be designed to address the full range of azimuthal effects imposed by the local geology and to collect additional free-field data..

ACKNOWLEDGMENTS

This work is sponsored by the Department of Energy, Office of Arms Control and Non-Proliferation (DOE/AN). We gratefully acknowledge the contribution of Tim Hall, the manager of the Grefco mine without whose help and cooperation these experiments could never have taken place. We also appreciate the help of Steve Woodard of Woodard Explosives for his help in the set up and detonation of the explosive charges. We also appreciate the

contributions of Harry Plannerer for the physical properties characterization, Jim Kamm for the modeling to help design the experiments, and Allen Cogbill for the seismic reflection surveys (all in the Geophysics Group at Los Alamos). The efforts of Bob Reinke and Al Leverett (DNA, Albuquerque), in the collection and analysis of the data for several of the experiments is gratefully acknowledged.

Table 1. Physical Property Determinations for the Dicaperl Perlite.

Physical Property	Mean	Range	Comments
Moisture (ASTM D2216)	0.27%	0.23% - 0.29%	crushed spec.
Moisture (ASTM D2216)	0.25%	0.16% - 0.37%	bulk specimens
Dry Bulk Density (ASTM C20)	1.86 g/cm ³	1.83 - 1.93 g/cm ³	
Grain Density (He pycnometer)	2.350 g/cm ³	2.341 - 2.359 g/cm ³	
Total Porosity (Calc.)	20.9%		

Table 2. Elastic Properties and Compression Test Parameters for the Dicaperl Perlite (ASTM D3148; D2216).

Specimen	$\Delta\sigma$ (kbars)	σ_3 (kbars)	E(kbars)	ν	Moisture (% total mass)
σ_1 perpendicular to flow banding ($\sigma_{1\perp}$):					
Perlit1S	0.249	0.0	174.3	0.13	0.19
Perlit2S	0.280	0.0	171.3	0.18	0.16
Perlit4S	0.280	0.0	119.3	0.07	0.68
Perlit6S	0.247	0.0	123.3	0.08	0.40
σ_1 in the plane of the flow banding ($\sigma_{1\parallel}$):					
Perlit3S	0.311	0.0	246.9	0.32	0.20
Perlit5S	[0.470]	0.0	240.0	0.20	2.90
Perlit5S#2	0.554	0.0	280.4	0.29	2.90
Perlit7S	0.367	0.0	nd	nd	0.86

$\Delta\sigma$ - maximum differential stress. ν - Poisson's ratio.
 σ_3 - confining stress. nd - not determined.
E - Young's modulus.
[] - maximum stress in a load/unload cycle without failure.

Table 3. Laboratory Determinations for the Perlite Compressional Wave Velocity.

Specimen	Path Orientation	Velocity (km/s)
P4-1	Vp \perp	3.08
P4-2	Vp \perp	3.14
P4-3	Vp \perp	2.94
P8-1	Vp \parallel	5.24
P8-2	Vp \parallel	5.25
P8-3	Vp \parallel	5.27

Path orientations:

Vp \perp - perpendicular to flow banding

Vp \parallel - parallel to flow banding

Table 4. Shot Summary[†].

Shot	Easting	Northing	Elevation	Explosive Charge	SDOB [‡] m/kg ^{1/3}	Comments
P1	29.5	24.5	1528.7	2.3 kg ANFO	1.8	RETARC
P2	30.2	36.9	1528.5	2.3 kg ANFO	1.6	RETARC
P3	29.4	13.7	1528.6	2.3 kg ANFO	1.1	CRATER
P4	30.7	48.3	1527.8	2.3 kg ANFO	2.0	Radial cracks
P5	30.4	59.5	1527.6	2.3 kg ANFO	2.3	No surface effects
P6	29.2	53.4	1527.6	1.8 kg ANFO	1.0	CRATER
P7	29.3	68.1	1527.4	1.1 kg ANFO	1.0	CRATER
P8	22.9	-49.0	1533.7	68.0 kg Petrogel	6.5	No surface effects
P9	0.0	0.0	1532.1	68.0 kg Petrogel	9.9	No surface effects
P10	0.0	0.0	1532.0	68.0 kg Petrogel	7.3	No surface effects
P11	0.0	0.0	1532.0	68.0 kg Petrogel	2.1	Minor surface cracks
P12	30.0	5.3	1529.5	68.0 kg Petrogel	3.4	No surface effects
P13	-34.7	-14.8	1534.1	68.0 kg Petrogel	2.9	No surface effects

[†]Coordinates are in meters relative to the surface ground zero of experiments P9-P11.

[‡]Scaled Depth of Burial.

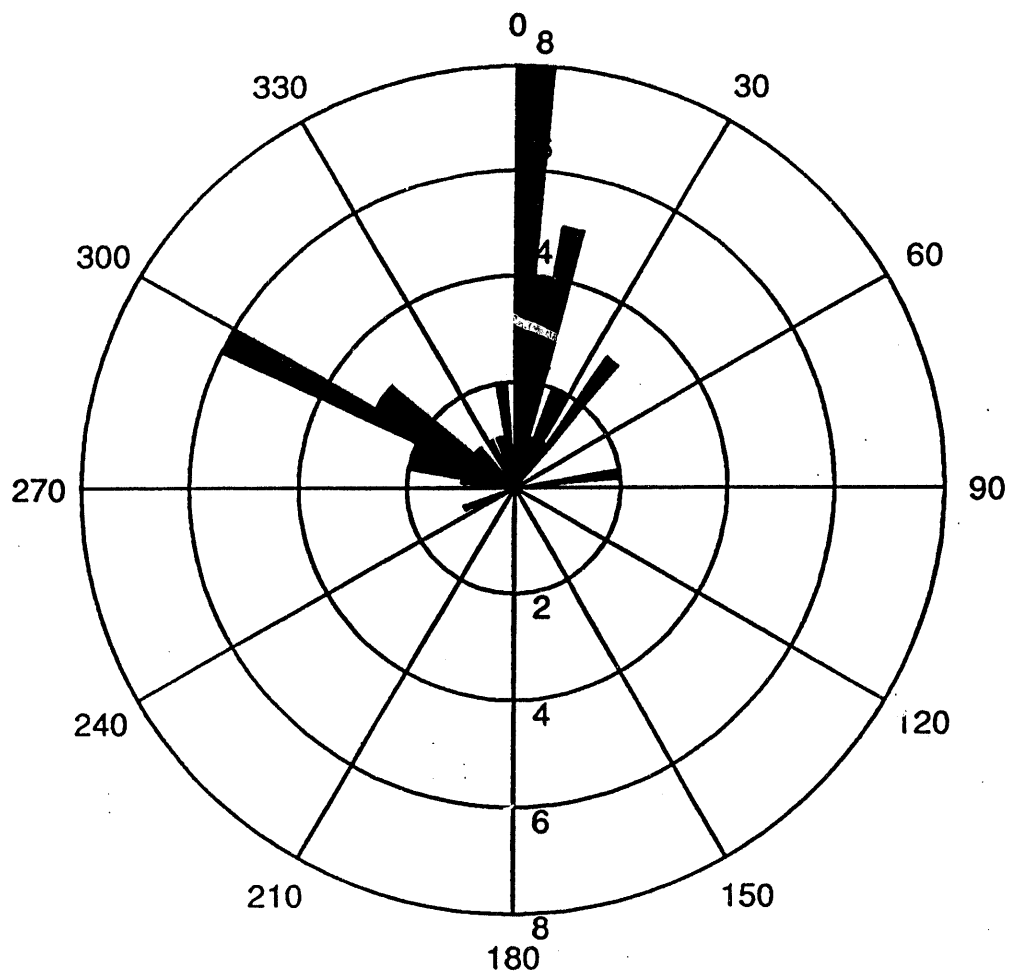


Figure 1. Rose diagram of exposed surface joints at the Grefco Dicaperl Mine. True north is indicated by 0° - east at 90° - south at 180° - west at 270°. Five degree bins were sampled. Major joint orientations at 0-15° (N-S) and 290-305° (WNW-SES).



Figure 2. Experiment layout. The squares are station locations and the crosses are the shots.

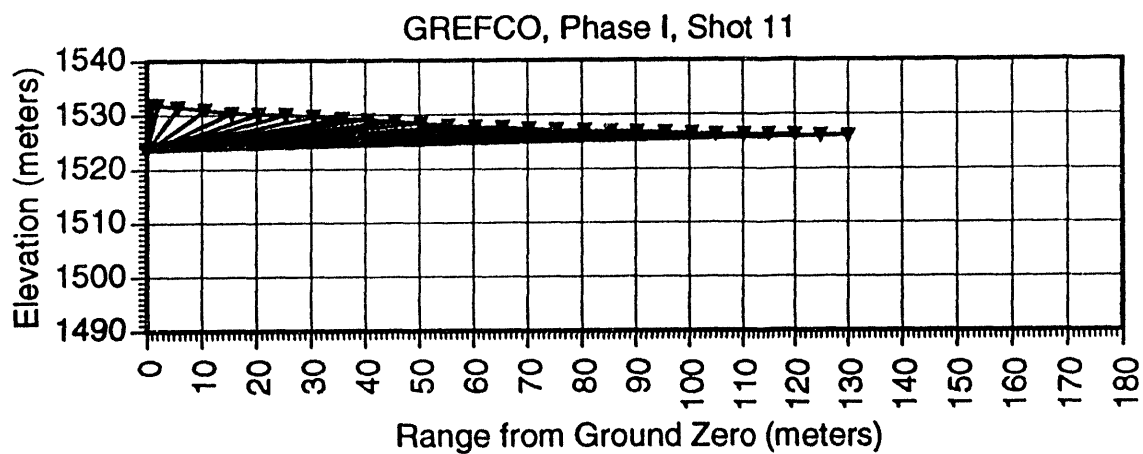
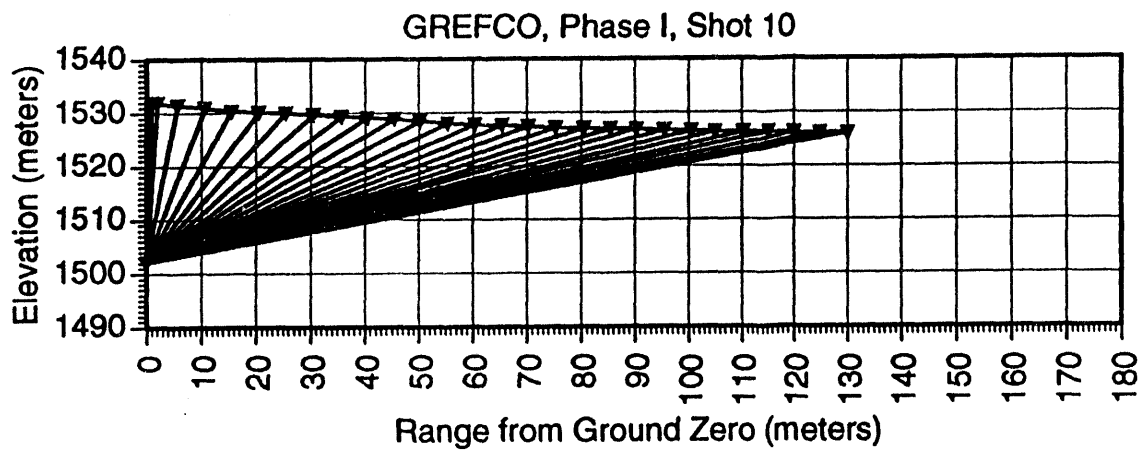
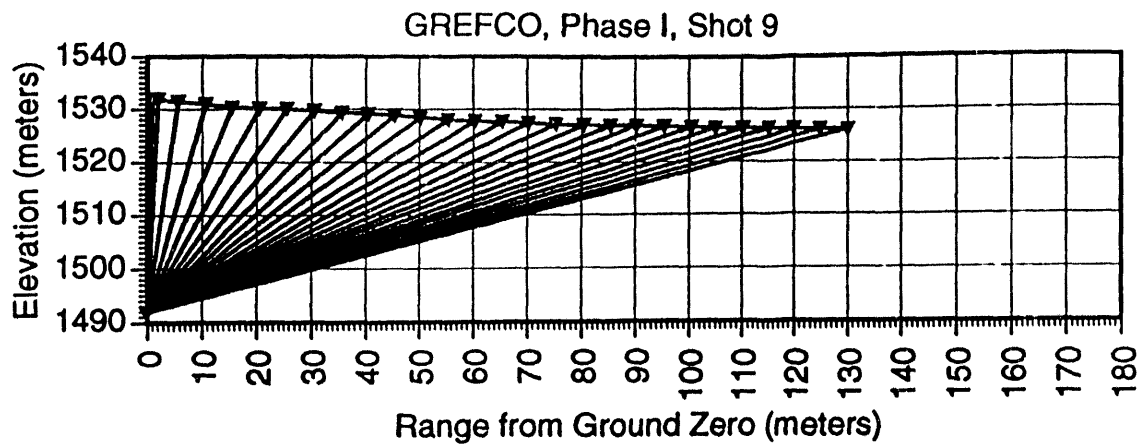


Figure 3. Ray path geometry for shots P-9 (a), P-10 (b), and P-11 (c). The shot depth of burial (DOB) strongly affects the incidence angle of the wave-front at the stations composing the long linear array (see Figure 1).

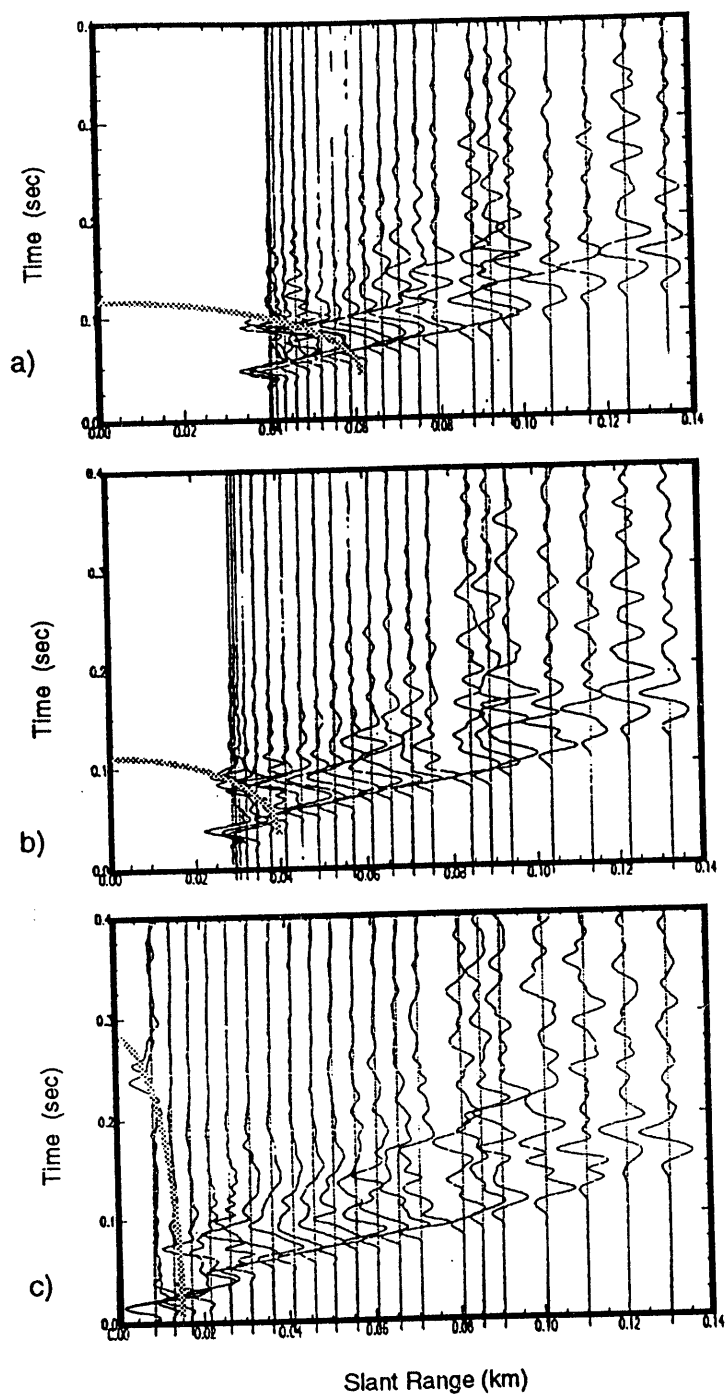


Figure 4. Record section plots of surface acceleration along the length of the Grefco Dicaperl test bed (see the long linear array in Figure 1). The data are presented as a function of slant range to facilitate determination of seismic velocities. The observed extent of surface spall is denoted by the hatched line. a) P-9 record section (DOB 40 m). b) P-10 record section (DOB 30 m). c) P-11 record section (DOB 10 m).

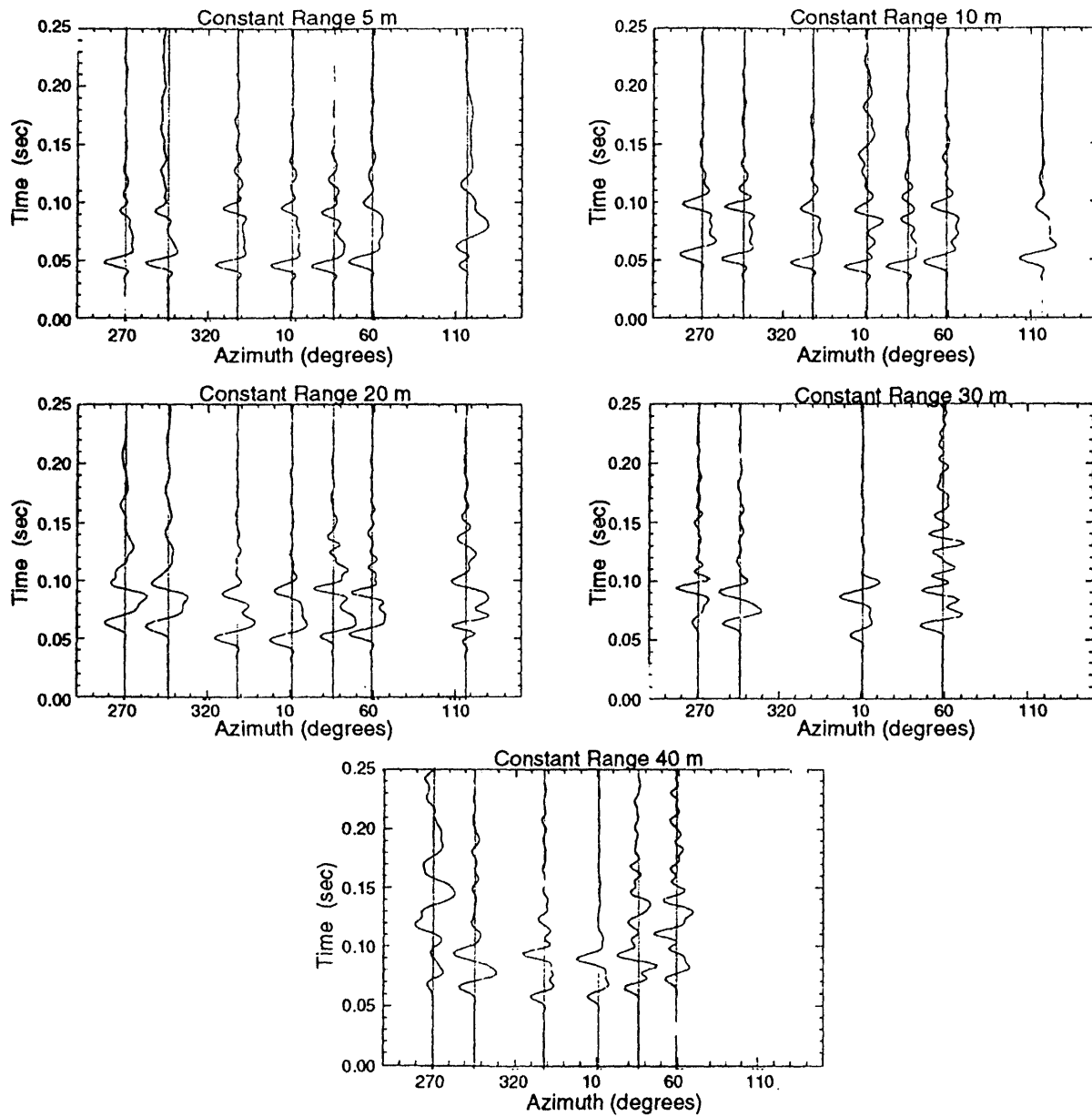


Figure 5. The azimuthal variation of the waveforms is shown for a) 5 meter range, b) 10 meter range, c) 20 meter range, d) 30 meter range, and e) 40 meter range. At 5 meters, the spall initiation time is nearly identical at all azimuths. At increasing ranges, the first motion is delayed in time at increasing and decreasing angles away from the major joint orientation near 0 degrees (see Figure 1). Spall dwell time decreases both with increasing range and increasing azimuth away from the major joint orientation.

DATE

FILMED

5/26/94

END

